VLBI With GNSS-signals on an Intercontinental Baseline – A progress report

R. Haas, T. Hobiger, G. Klopotek, N. Kareinen, J. Yang , L. Combrinck, A. de Witt, M. Nickola

Abstract VLBI-observations of GNSS-signals have been discussed for several years as a apossible approach to improve the accuracy of the terrestrial reference frame. Several experimental observing sessions have been performed during the last years, primarily with regional VLBI networks in Europe and Australia. Here we present VLBI observations of GNSS-signals performed on an intercontinental baseline between Onsala (Europe) and Hartebeesthoek (Africa). These observations are part of a ESA pilot project within the Alcantara programme of the European Space Agency (ESA) and aim at achieving synergies between VLBI and GNSS. Data were collected during several sessions in 2017, successfully correlated and post-processed, and analyzed with a geodetic VLBI data analysis software. The results show that ... We briefly describe these sessions, and present first preliminary results.

Keywords VLBI, GNSS, satellite observations, DiFX, Fourfit, C5++

1 Introduction

A global geodetic terrestrial reference frame, such as the international terrestrial reference frame (ITRF) (Altamimi et al., 2011, 2016) is of great importance for society (United Nations, 2015). However, the current quality of the global terrestrial reference frame is regarded as still being insufficient for studies concerning global change processes, such as sea level rise (Blewitt et al., 2010). In particular the quality of the so-called local ties at co-location stations is often suspected to be the reason for the insufficient qualify of the ITRF (Altamimi et al., 2011; Seitz et al., 2012).

As one promising approach to improve the consistency and accuracy of the global terrestrial reference frame the idea of co-location onboard satellites has been proposed (Rothacher et al., 2009). This includes dedicated multi-technique co-location satellites such as the Chinese APOD (Tang et al., 2016) or the proposed E-GRASP satellite (Biancale et al., 2017), but involves also VLBI observations of GNSS satellites. Concerning the latter, simulation studies performed by Plank et al. (2014) showed promising results for VLBI observations of GPS satellites in a seven station European VLBI network, providing 3D station position repeatabilities on the order of 5–10 mm.

Test observations of GNSS signals were performed during the last years mainly with VLBI stations in either Europe or Australia. Often observations were performed on a single baseline only. The stations involved were primarily Onsala, Medicina, Noto, Wettzell in Europe, e.g. (Tornatore et al., 2011; Haas et al., 2014, 2015) and Hobart and Ceduna in Australia (Plank et al., 2017).

These stations involved are equipped with L-band receiving systems, the European stations with dual circular polarisation, and the Australian ones with dual linear polarisation. Most of the L-band systems are bandwidth restricted, i.e. it is not possible to observe simultaneously both the GPS L1 (1575.42 MHz) and L2 (1227.60 MHz) frequency bands. Often the GPS L2 is even out of the receiver capabilities, and form some even GPS L1 is difficult to reach. However, for the latter at least the GLONASS L1 (1600 MHz) was reachable.

Most of the telescopes involved do not yet allow continuous tracking of orbiting objects, so that a stop-and-go type of observing strategy with update intervals on the order of 10 s to 15 s had to be used to follow the satellites.

Inspired by the promising simulation study (Plank et al., 2014) and the successful test observations (Tor-

---

Rüdiger Haas · Thomas Hobiger · Grzegorz Klopotek · Niko Kareinen · Jun Yang
Chalmers University of Technology, Department of Space, Earth and Environment, Onsala Space Observatory, SE–439 92 Onsala, Sweden

Ludwig Combrinck · Alet de Witt · Marisa Nickola
Hartebeesthoek Radio Observatory, Krugersdorp, 1740, South Africa

natore et al., 2011; Haas et al., 2014, 2015; Plank et al., 2017), ESA initiated a called for a pilot project within its Alcantara programme on the topic of Synergies between VLBI and GNSS. The goals of this pilot project are to study whether VLBI observations of GNSS signals really can be used to improve the terrestrial reference frames, to test intercontinental networks, and in particular the impact of Galileo. We submitted a proposal to this call and were lucky to get a contract for this pilot project.

2 Observations

As part of the ESA pilot project, we performed in 2017 a number test experiments on the Onsala – Hartebeesthoek baseline. The telescopes used are the 25 m radio telescope at Onsala (ONSALA85) usually used for astronomical VLBI, and the 26 m radio telescope at Hartebeesthoek (HARTRAO) which is used for both geodetic and astronomical VLBI. While ONSALA85 was involved in the first intercontinental geodetic VLBI observations in the late 1960'ies and has been observing the S-band part of geodetic S/X measurements together with the Onsala 20 m telescope (ONSALA60), which did the X-band part, in the late 1970'ies, it has not been used for geodetic VLBI since then. The station coordinates of ONSALA85 were determined from local tie measurements (Lundqvist, 1982) and VLBI at C-band (Charlot et al., 2001). HARTRAO on the other hand is regularly used in geodetic VLBI in the IVS observing programme and thus should have updated and reliable coordinates.

Between January and July 2017 we organised in total eight so-called OHT-sessions. The backbone of these sessions is the Onsala-Hartebeesthoek baseline. Since the aim of the pilot project was to do real network observations, we tried to include additionally further telescopes. For the most recent sessions in May and July we were able to include additionally the Russian station Zelenchukskaya. This station is also regularly participating in the geodetic VLBI observing plan and has well established coordinates and promises to improve the observing geometry.

The observing plans were scheduled with the VieVs scheduling tool (Hellerschmied et al., 2015). The first tests were done focussing on to observe GPS satellites. Then we also included GLONASS observations. However, we realized soon that the inclusion of GLONASS caused difficulties due to the necessity to adjust the observation frequency bands. Thus, we left the idea of combined GPS and GLONASS observations again. Instead, we added Galileo to the observing plan for the more recent sessions. Galileo satellites also use the same L1 center frequency as GPS, though the signal characteristics are quite different.

Table 1 gives an overview of the so-far performed OHT-sessions, with their dates, durations, participating stations and GNSS observed. In the sequence of this manuscript we will concentrate on the first three sessions which involved one intercontinental baseline only.

Table 1: Overview of the VLBI sessions

Session	date	duration	stations	satellites
OHT1	2017-01-24	1 h	O8 - Hh	GPS
OHT2	2017-01-31	4 h	O8 - Hh	GPS + GLONASS
OHT6	2017-04-07	4 h	O8 - Hh	GPS + Galileo
OHT7	2017-05-22	2.5 h	O8 - Hh - Zc	GPS + Galileo
OHT8	2017-07-24	24 h	O8 - Hh - Zc	GPS + Galileo

The setup chosen for the OHT experiments was to observe four channels of 16 MHz bandwidth (for OHT6 32 MHz), two in each polarisation, centered on the GPS/Galileo L1 center frequency. For OHT2 the observing frequencies were adapted to the corresponding GLONASS satellites, and on GPS L1 for GPS satellites. Except for OHT1, also natural radio sources were observed, typically at the beginning and the end of the session and in regular intervals during the session. These radio sources were rather near by the satellites, Therefor the observing frequencies for the radio sources were slightly offset in order to avoid potential leaking of satellite signals through e.g. side lobes.

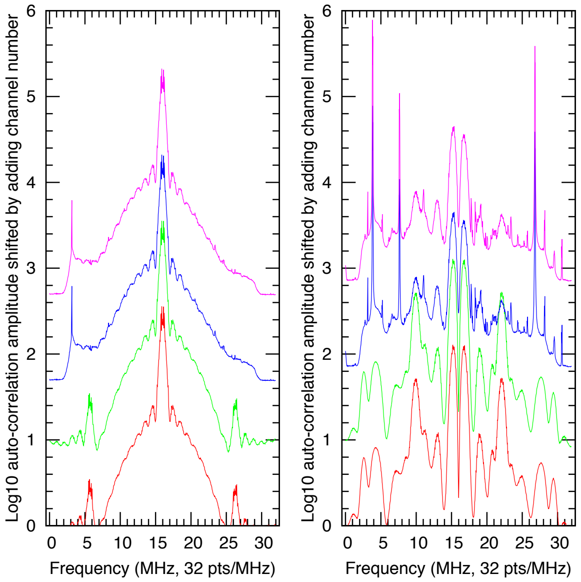

Fig. 1: Examples of spectra observed locally at Onsala during session OHT6: Bandpass of a GPS satellite (left) and a Galileo satellite (right). Shown are four channels covering 32 MHz.

The plots presented in Fig. 1 are examples of the spectra locally observed at Onsala during OHT6. Shown are 4 observing channels of 32 MHz bandwidth. The difference in the signal characteristics between GPS (left) and Galileo (right) is clearly visible.

3 Data processing

The observed raw data were e-transferred to Onsala and correlated there with the software correlator DiFX (Deller et al., 2011). The a priori delays necessary for the correlation of the satellite observations were determined with the C5++ software (Hobiger et al., 2010) using near-field modeling following Duev et al. (2012). Fringe-fitting was performed with the *Fourfit* program.

It turned out that the 10 s long scans gave rather high SNR values, on the order of 10000 and more. As an example the finge plot of GPS satellite PG03 observed during OHT1 is presented in Fig. 2. With 10 s of data SNR values of more than 11000 can be achieved. We thus decided to split up the data into smaller pieces of 1 s for the correlation and fringe fitting, which still provided sufficiently high SNR values.

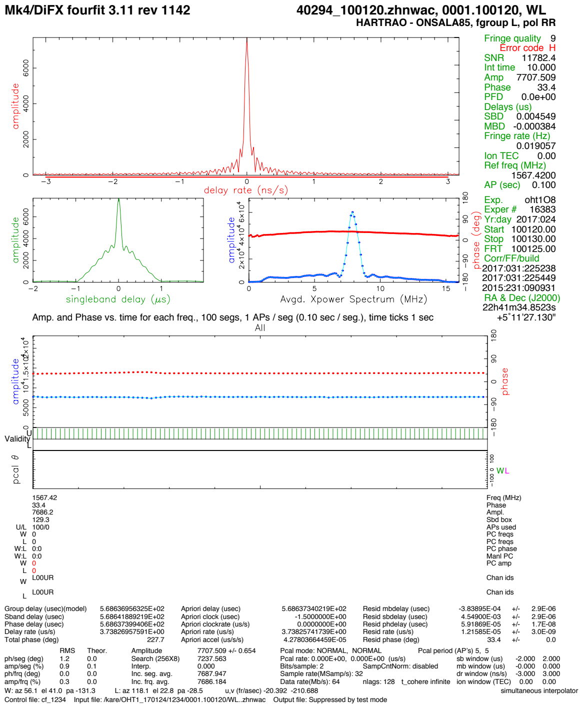
```
Mk4/DiFX fourfit 3.11 rev 1142                40294_100120.zhnwac, 0001.100120, WL
                                    HARTRAO - ONSALA85, fgroup L, pol RR

Fringe quality   9
     Error code  H
SNR        11782.4
Int time    10.000
Amp       7707.509
Phase         33.4
PFD       0.0e+00
Delays (us)
SBD       0.004549
MBD      -0.000384
Fringe rate (Hz)
          0.019057
Ion TEC       0.00
Ref freq (MHz)
         1567.4200
AP (sec)     0.100
Exp.        oht1O8
Exper #      16383
Yr:day    2017:024
Start    100120.00
Stop     100130.00
FRT      100125.00
Corr/FF/build
2017:031:225238
2017:031:225449
2015:231:090931
RA & Dec (J2000)
22h41m34.8523s
   +5°11'27.130"

Amp. and Phase vs. time for each freq., 100 segs, 1 APs / seg (0.10 sec / seg.), time ticks 1 sec

     1567.42                                   Freq (MHz)
     33.4                                      Phase
     7686.2                                    Ampl.
     129.3                                     Sbd box
U/L  100/0                                     APs used
  W  0                                         PC freqs
  L  0                                         PC freqs
W:L  0:0                                       PC phase
W:L  0:0                                       Manl PC
  W  0                                         PC amp
  L  0
     L00UR                                     Chan ids
  W
     L00UR                                     Chan ids
  L

Group delay (usec)(model)  5.68636956325E+02   Apriori delay (usec)        5.68637340219E+02   Resid mbdelay (usec)   -3.83895E-04  +/-  2.9E-06
Sband delay (usec)         5.68641889219E+02   Apriori clock (usec)       -1.5000000E+00       Resid sbdelay (usec)    4.54900E-03  +/-  2.9E-06
Phase delay (usec)         5.68637399406E+02   Apriori clockrate (us/s)    0.0000000E+00       Resid phdelay (usec)    5.91869E-05  +/-  1.7E-08
Delay rate (us/s)          3.73826957591E+00   Apriori rate (us/s)         3.73825741739E+00   Resid rate (us/s)       1.21585E-05  +/-  3.0E-09
Total phase (deg)                      227.7   Apriori accel (us/s/s)      4.27803664459E-05   Resid phase (deg)              33.4  +/-      0.0
               RMS   Theor.   Amplitude        7707.509 +/- 0.654   Pcal mode: NORMAL,  NORMAL        Pcal period (AP's) 5,  5
ph/seg (deg)   1.2   0.0      Search (256X8)   7237.563             Pcal rate: 0.000E+00,  0.000E+00  (us/s)   sb window (us)   -2.000  2.000
amp/seg (%)    0.9   0.1      Interp.          0.000                Bits/sample: 2      SampCntNorm: disabled  mb window (us)   -0.000  0.000
ph/frq (deg)   0.0   0.0      Inc. seg. avg.   7687.947             Sample rate(MSamp/s): 32                   dr window (ns/s) -3.000  3.000
amp/frq (%)    0.3   0.0      Inc. frq. avg.   7686.184             Data rate(Mb/s): 64   nlags: 128   t_cohere infinite   ion window (TEC)  0.00  0.00
W: az 56.1  el 41.0  pa -131.3     L: az 118.1  el 22.8  pa -28.5     u,v (fr/asec) -20.392  -210.688                simultaneous interpolator
Control file: cf_1234    Input file: /kare/OHT1_170124/1234/0001.100120/WL..zhnwac    Output file: Suppressed by test mode
```

Fig. 2: Fringe plot for GPS satellite PG03 observed on the baseline Onsala-Hartebeesthoek during session OHT1.

4 Preliminary results

After correlation and fringe fitting the resulting delay values were analysed using the C5++ software. Standard routines were used for the processing. Tropospheric information was used based on the GPT2 model and ionospheric corrections were applied based on global TEC maps provided by the IGS.

Since HartRAO is an active IVS station with well established coordinates in the ITRF it was used as reference station for the data analysis, both concerning the station position as well as concerning the reference clock. Station position corrections were estimate for ONSALA85, as well as clock offsets and rates. For both station involved in the sessions, zenith wet delay (ZWD) and station-dependent ionospheric biases were estimated. Additionally, for each satellite observed, a satellite-specific time bias was estimated. The latter were introduced to partly take care ionospheric influences, as well as instrumental delays due to the interaction of individual satellite signal structure and filter characteristics of the receiving systems.

Unfortunately, the ionospheric corrections based on global TEC maps do not give sufficient detail and thus do not sufficiently remove the ionospheric effects from the observed single frequency delays. As a consequence, the other parameters that are estimated in the data analysis will partly be absorbing remaining ionospheric contributions. Therefore it is not meaningful yet to investigate the estimated parameters in detail.

Instead, as a quality measure, we have a look at the post-fit residuals of the first three sessions. The post-fit residuals of OHT1, OHT2 and OHT3 are presented in Fig. 3, Fig. 4, and Fig. 5, respectively

It becomes evident that there are still systematics left in the residuals. There is e.g. a kind of ”saw-tooth” pattern within the 5 minutes long observing epochs per

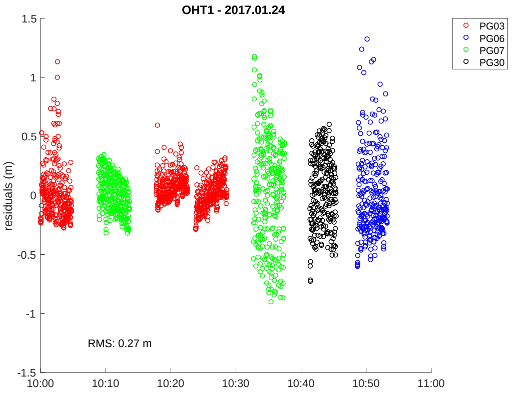

Fig. 3: Post-fit residuals for OHT1.

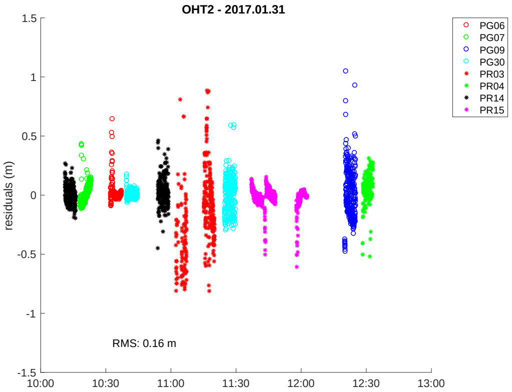

Fig. 4: Post-fit residuals for OHT2.

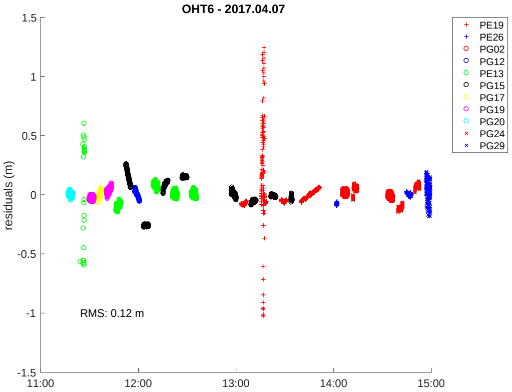

Fig. 5: Post-fit residuals for OHT6.

satellite (see e.g. PG07 in Fig.3). This might be related to the stop-and-go type of observation strategy where the telescopes were repointed every 10 s to follow the satellite passes. There are also ”satellite jumps” visible, both between different satellites, but also when coming back to the same satellite (see e.g. PG03 and PG07 in Fig. 3, or PG06 in Fig. 4, or PG13 in Fig. 5). Sometimes there are ”satellite patterns”, i.e. residuals fading in or fading out (see e.g. PR15 in Fig. 4), probably due to tracking issues. And sometimes satellites show rather large residuals due to so far unknown reasons (see e.g. PE19 in Fig. 5). Thus, more work is needed in order to understand these features. Table 2 provides some statistical information on the analysis of all three stations.

Table 2: Statistics for the first three OHT sessions

Session	duration	observations	post-fit RMS (m)
OHT1	1 h	1948	0.27
OHT2	4 h	3340	0.16
OHT6	4 h	5144	0.12

5 Conclusions

During 2017 we performed a serie of successful VLBI observations of GNSS signals on an intercontinental baseline between Onsala and Hartebeesthoek. Signals of GPS, GLONASS and Galileo satellites were observed and correlated. Even with data sets as short as 1 s sufficiently high SNR is achieved.

The geodetic analysis of these data was done with C5++ and a number of parameters were estimated, including station position, station clock parameters, and troposphere parameters. The lack of ionospheric correction with sufficient detail and accuracy leads to that the estimated parameters are influenced by these remaining ionospheric effects. The post-fit residuals are on the order of 12-27 cm. However, a number of systematic effects are left in the post-fit residuals, e.g. a ”saw-tooth” pattern within the satellite scans, and ”satellite jumps”. So, more work is needed to understand these systematics and to improve the performance. Further observing sessions, preferably including more stations and with at least 24 h observation time are planned to address these issues. One aspect that in particular requires improvement is the handling of ionospheric effects.

However, in general, we think that the approach to observe GNSS-signals with VLBI radio telescopes is promising. We thus support the ideas of to equip one or several of the second generation Galileo satellites with artificial senders for VLBI observations.

References

Altamimi Z, Collilieux X, M7'e9tivier L (2011) ITRF2008: an improved solution of the international terrestrial reference frame. *J Geod*, 85(8), 457–473,

Altamimi Z, Rebischung P, Métivier L, Xavier C (2016) ITRF2014: A new release of the International Terrestrial Reference Frame modeling nonlinear station motions. *J. Geophys. Res. Solid Earth*, 121, 6109–6131, {doi:10.1002/2016JB013098

Biancale R, Pollet A, Coulot D, Mandea M (2017) E-GRASP/Eratosthenes: a mission proposal for millimetric TRF realization. *Geophysical Research Abstracts*, 19, EGU2017-8752.

Blewitt G, Altamimi Z, Davis J, Gross R, Kuo C Y, Lemoine F G, Moore A W, Neilan R E, Plag H-P, Rothacher M, Shum C K, Sideris M, Schöne T, Tregoning P, Zerbini S (2010) Geodetic Observations and Global Reference Frame Contributions to Understanding Sea-Level Rise and Variability. In: J. A. Church, P. L. Woodworth, T. Aarup, W. S. Wilson (eds.), Understanding Sea-Level Rise and Variability, 1st edition, Blackwell Publishing Ltd., 256–284, doi:10.1002/9781444323276.ch9

Charlot P, Campbell R, Alef W, Borkowski K, Conway J, Foley A, Garrington S, Kraus A, Nothnagel A, Sovers O, Trigilio C, Venturi T, Xinyong H (2001) ITRF2000 Positions of

Non-geodetic Telescopes in the European VLBI Network. In: D. Behrend, A. Rius (eds.), *Proc. 15th Working Meeting on European VLBI*, 194–200.

Collilieux X, Wöppelmann G,(2011) Global sea-level rise and its relation to the terrestrial reference frame. *J Geod*, 85(1), 9–22, doi:10.1007/s00190-010-0412-4

Deller A T, Brisken W F, Phillips C F, Morgan J, Alef W, Cappallo R, Middelberg E, Romney J, Rottmann H, Tingay S J, Wayth R (2011) DiFX-2: A More Flexible, Efficient, Robust, and Powerful Software Correlator. *Pub Astron Soc Pac*, 123(901), 275–287.

Duev D A, Molera Calves G, Pogrebenko S V, Gurvits L I, Cimo G, Bahamon T B (2012) Spacecraft VLBI and doppler tracking: algorithms and implementation. *Astronomy & Astrophysics* 541, A43, doi:10.1051/0004-6361/201218885.

Haas R, Neidhardt A, Kodet J, Plötz Ch, Schreiber K-U, Kronschnabl G, Pogrebenko S, Duev D, Casey S, Marti-Vidal I, Yang J, Plank L (2014) The Wettzell-Onsala G130128 experiment – VLBI-observations of a GLONASS satellite. In: D. Behrend, K. D. Baver, K. L. Armstrong (eds.), *IVS 2014 General Meeting Proc.*, Science Press (Beijing), 451–455.

Haas R, Hobiger T, Hellerschmied A, Neidhardt A, Kodet J (2015) GLONASS-VLBI: Onsala-Wettzell test observations. In: R. Haas, F. Colomer (eds.), *Proc. 22nd EVGA Working Meeting*, 107–111.

Hellerschmied A, Böhm J, Neidhardt A, Kodet J, Haas R, Plank L (2015) Scheduling VLBI observations to satellites with VieVS. In: T. van Dam (ed.), *REFAG 2014, International Association of Geodesy Symposia 146*, doi:10.1007/1345_2015_183

Hobiger T, Otsubo T, Sekido M, Gotoh T, Kubooka T, Takiguchi H (2010) Fully automated VLBI analysis with c5++ for ultra rapid determination of ut1. *Earth Planets Space* 62, 993–937, doi:10.5047/eps.2010.11.008.

Lundqvist G (1982) Precision Surveying at the 1-mm level using radio interferometry. In: *Proc. Symposium No. 5-IAG*, NOAA Technical Report NOS 95 NGS 24, 99.

Plank L, Böhm J, Schuh H (2014) Precise station positions from VLBI observations to satellites: a simulation study. *J Geod* 88(7):659–673, doi:10.1007/s00190-014-0712-1

Plank L, Hellerschmied A, McCallum J, Böhm J, Lovell J (2017) VLBI observations of GNSS-satellites: from scheduling to analysis. *J Geod* 91(7):867–880, doi:10.1007/s00190-016-0992-8.

Rothacher M, Beutler G, Behrend D, Donnellan A, Hinderer J, Ma C, Noll C, Oberst J, Pearlman M, Plag H-P, Richter B, Schöne T, Tavernier G, Woodworth P (2009) The future global geodetic observing system. In: H.-P. Plag, M. Pearlman (eds.), Global Geodetic Observing System - Meeting the Requirements of a Global Society on a Changing Planet in 2020. Springer, 237–272, doi:10.1007/978-3-642-02687-4

Seitz M, Angermann D, Bloßfeld M, Drewes H, Gerstl M (2012) The 2008 DGFI realization of the ITRS: DTRF2008. *J Geod*, 86(12), 1097–1123.

Tang G, Sun J, Li X, Liu S, Chen G, Ren T, Wang G (2016) APOD Mission Status and Observations by VLBI. In: D. Behrend, K. D. Baver, K. L. Armstrong (eds.), *IVS 2016 General Meeting Proceedings - "New Horizons with VGOS"*, NASA/CP-2016-219016, 363–367.

Tornatore V, Haas R, Duev D, Pogrebenko S, Casey S, Molera Calvés G, Keimpema A (2011) Single baseline GLONASS observations with VLBI: data processing and first results. In: W. Alef, S. Bernhart, A. Nothnagel (eds.), *Proc. 20th EVGA Working Meeting*, 162–165.

United Nations General Assembly (2015) UN General Assembly resolution: A global geodetic reference frame for sustainable development. `http://www.un.org/ga/search/view_doc.asp?symbol=A/69/L.53`

Schaer S, Beutler G, Rothacher M, Springer T A (1996) Daily global ionosphere maps based on GPS carrier phase data routinely produced by the CODE. In: R. E. Neilan, P. A. Van Scoy, J. F. Zumberge (eds.), *Pro. IGS Analysis Center Workshop*, International GNSS Service. 181–192.

Sekido M, Kondo T, Kawai E, Imae M (2003) Evaluation of GPS-based ionospheric TEC map by comparing with VLBI data. *Radio Science* 38, doi:10.1029/2000RS002620.